illustrates the importance of including the orthotropicity of the material in analyses.

References

[1] Woinowski-Krieger, S., "Buckling Stability of Circular Plates with Circular Cylindrical Aeolotropy," *Ingenieur-Archiv*, Vol. 26, 1958, pp. 129–131.

[2] Mossakowski, J., "Buckling of Circular Plates with Cylindrical Orthotropy," *Archiwum Mechaniki Stosowanej*, Vol. 12, 1960, pp. 583–596.

[3] Pandalai, K. A. V. and Patel, S. A., "Buckling of Orthotropic Circular Plates," *Journal of the Royal Aeronautical Society*, Vol. 69, April 1965, pp. 279–280.

[4] Uthgenannt, E. B., "Buckling and Nonlinear Behavior of Orthotropic Annular Plates," Ph.D. thesis, June 1970, University of Connecticut, Storrs, Conn.

[5] Hildebrand, F. B., *Methods of Applied Ma'hematics*, 2nd ed., Prentice-Hall, New Jersey, 1965, pp. 62–65.

[6] Schubert, A., "Kleine Mitterlungen," *Zeitschrift fur angewandte Mathematik und Mechanik*, Vol. 25/27, No. 4, July 1947, pp. 123–124.

[7] Yamaki, N., "Buckling of a Thin Annular Plate Under Uniform Compression," *Journal of Applied Mechanics*, Vol. 25, June 1958, pp. 267–273.

[8] Meissner, E., "Ueber das Knicken kreisring formiger Scheiben," *Schweiz Bauzeitung*, Vol. 101, No. 8, Feb. 1933, pp. 87–89.

[9] Rozsa, M., "Stability Analysis of Thin Annular Plates Compressed Along the Outer or Inner Edge by Uniformly Distributed Radial Forces," *Acta Technica Academiae Scientiarum Hungaricae*, Vol. 53, 1966, pp. 359–377.

Sphere Drag in Near-Free-Molecule Hypersonic Flow

M. I. Kussoy,* D. A. Stewart,* and C. C. Horstman†
NASA Ames Research Center, Moffett Field, Calif.

THERE are many practical applications, such as satellite drag and lifetime predictions, and density measurements in the upper atmosphere where a precise knowledge of the drag coefficient (C_D) of spheres at hypersonic Mach numbers for near-free-molecule flow conditions is required. Recent experimental investigations[1–5] have measured drag coefficients in near-free-molecular flow equal to or slightly less than the free-molecule limit (assuming diffuse reflection and an accommodation coefficient of one). These data were obtained for both hot- and cold-wall conditions at Mach numbers from 8 to 15. A few experiments at $M_\infty > 15$ by Slattery et al.,[1] and Kussoy and Horstman[6] have indicated

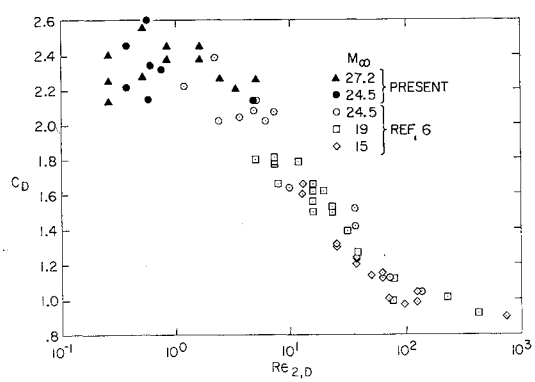

Fig. 1 Sphere-drag coefficient variation with Reynolds number.

Received June 24, 1970; revision received August 3, 1970.

* Research Scientist. Member AIAA.

† Research Scientist. Associate Eellow AIAA.

Table 1 Sphere drag-coefficient results

Condition 1: $M_\infty = 27.2$, $Re_\infty/\text{cm} = 221$, $Re_2/\text{cm} = 6.6$, $T_w/T_0 = 0.035$, $T_w/T_\infty = 5.3$, $T_w = 294°\text{K}$		Condition 2: $M_\infty = 24.5$, $Re_\infty/\text{cm} = 236$, $Re_2/\text{cm} = 9.4$, $T_w/T_0 = 0.035$, $T_w/T_\infty = 4.1$, $T_w = 294°\text{K}$	
Sphere diam., cm	C_D(meas.)	Sphere diam., cm	C_D(meas.)
0.762	2.26	0.559	2.13
0.559	2.20	0.080	2.31
0.376	2.26	0.064	2.34
0.254	2.45, 2.37	0.061	2.60, 2.14
0.130	2.45, 2.37	0.041	2.45, 2.21
0.080	2.55, 2.27		
0.040	2.40, 2.25, 2.13		

sphere drag coefficients above their free molecule limits. The purpose of this Note is to present additional data in the near-free-molecular regime for flow conditions ($M_\infty \approx 25$, $T_w/T_\infty \approx 5$) which are closer to Earth satellite conditions.

The present data were obtained using a free-flight technique in the Ames 42-in. Shock Tunnel. The operation and calibration procedures of this facility are described elsewhere.[6] The present test conditions are given in Table 1. The free-flight technique is similar to that used in Ref. 6, except for the model launch procedure which employed a retractable table similar to the one described in Ref. 7. The accuracy of the data have been calculated to be $\pm 10\%$ for the present investigation. The larger spheres (0.76–0.25 cm diam) were made from maple, pine, balsa wood, steel, zinc, copper, or plastic, and spray-painted with black paint. The smaller spheres (0.041–0.25 cm diam) were made from a synthetic sapphire-ruby material and painted with a diluted blue marking dye solution. Within experimental accuracy, no effect of surface or material on the drag could be observed.

The sphere drag results for air are presented in Table 1 and are shown on Fig. 1, plotted against $Re_{2,D}$ (the Reynolds number based on conditions behind the bow shock wave). Results obtained previously[6] are also shown. At comparable Reynolds numbers, they are in good agreement with the present results. At values of $Re_{2,D} < 1$, the drag coefficient levels off to an average value of 2.35 which is 10% above the free-molecular drag coefficient (2.12) computed for the present test conditions assuming diffuse reflection and an accommodation coefficient of one.

Hersh[2] showed that this higher drag coefficient was theoretically plausible if the energy accommodation coefficient was less than one. Free-molecule sphere drag coefficients up to 2.6 could be computed for the present test conditions assuming energy accommodation was less than one. In a similar vein, Hurlbut and Sherman,[8] using a reflection model originally proposed by Nocilla,[9] computed theoretical values of the free-molecule drag coefficient for spheres in hypersonic flow ranging from below 2.0 to about 2.8, depending on the particular reflection model chosen. It is likely that the reason for the present data being above the "free-molecule limit" while the previous data[1–5] are close to or below their "free-molecule limits," is because of the differences between the surface reflection and/or energy accommodation laws as a function of Mach number and wall temperature ratio in this flow regime. However, it is not possible to determine the particular reflection laws and coefficients from these experimental results because of the integration process involved.[2,8] Thus, for problems such as predictions of satellite lifetimes and atmospheric density measurements, the experimental sphere drag coefficients should be used whenever possible.

References

[1] Slattery, J. C., Friichtenicht, J. F., and Hamermesh, B., "Interaction of Micrometeorites with Gaseous Targets," *AIAA Journal*, Vol. 2, No. 3, March 1964, p. 543.

[2] Hersh, A. S., Friichtenicht, J. F., and Slattery, J. C., "Drag Coefficients of Microscopic Spheres in Free Molecule Flow," *Rarefied Gas Dynamics Supplement 5*, edited by L. Trilling and H. Wachman, Academic Press, New York, 1969.

[3] Potter, J. L. and Miller, J. T., "Sphere Drag and Dynamic Simulation in Near-Free-Molecular Flow," *Rarefied Gas Dynamics*, edited by L. Trilling and H. Y. Wachman, Academic Press, New York, 1969.

[4] Smolderen, J. J. et al., "Sphere and Cone Drag Coefficients in Hypersonic Transitional Flow," *Rarefied Gas Dynamics*, edited by L. Trilling and H. Y. Wachman, Academic Press, New York, 1969.

[5] Phillips, W. M. and Kuhlthau, A. R., "Drag Measurements on Magnetically Supported Spheres in Low Density High Speed Flow," *Rarefied Gas Dynamics*, edited by L. Trilling and H. Y. Wachman, Academic Press, New York, 1969.

[6] Kussoy, M. I. and Horstman, C. C., "Cone Drag in Rarefied Hypersonic Flow," *AIAA Journal*, Vol. 8, No. 2, Feb. 1970, p. 315.

[7] Geiger, R. E., "Slender Cone, Zero Angle-of-Attack Drag in Continuum and Noncontinuum Flow," AIAA Paper 69-711, San Francisco, Calif. 1969.

[8] Hurlbut, F. C. and Sherman, F. S., "Application of the Nocilla Wall Reflection Model to Free-Molecule Kinetic Theory," *The Physics of Fluids*, Vol. 11, No. 3, March 1968.

[9] Nocilla, S., "The Surface Re-Emission Law in Free Molecule Flow," *Rarefied Gas Dynamics*, edited by J. A. Laurmann, Academic Press, New York, 1963.

A Method of Curvature Matching for Two-Dimensional Flexible Plate Wind-Tunnel Nozzles

S. S. Desai* and R. K. Jain*
National Aeronautical Laboratory, Bangalore, India

Nomenclature

A = area under the aerodynamic K-S plot
E = Young's modulus of elasticity
I = moment of inertia of the plate cross section
K = curvature
m = slope of the linear K-S plot
R = total load applied on a jack
S = distance along the plate
$[A]$ = area matrix
$[C]$ = coefficient matrix
$[K]$ = unknown curvature matrix

Subscripts

i = ith station on the plate contour
av = average

Introduction

In order to simulate the contour of a two-dimensional wind-tunnel nozzle for continuously varying test section Mach number, it is usual to employ two flexible plates loaded transversely by a finite number of jacks along its length. It is impossible to exactly simulate the aerodynamic contour by the device previously mentioned. If the jack extensions are adjusted to make the ordinates of the plate at a finite number of points equal to those of the aerodynamic contour at these points, the slope and the curvature distributions of the plate deviate from those of the contour, resulting in nonuniformity in the Mach number distribution in the test section. For obtaining a uniform Mach number distribution, it is necessary to simulate the slope distribution exactly.

It may be noted that the exact simulation of the slope distribution throughout the plate length is impossible. For practical purposes, it is sufficient to ensure identical slopes at the finite number of points. This can be done by matching the curvature distribution of the plate with that of the aerodynamic contour.

This Note describes a method of curvature matching adopted for the nozzle contours of the 4 ft × 4 ft trisonic wind tunnel of National Aeronautical Laboratory, India (NAL). As a consequence of matching, a set of over-determined, simultaneous equations is obtained. A least-square solution of these equations gives the curvature distribution which ensures minimum slope error.

The analysis for the derivation of this set of equations follows.

Analysis

The arrangement of the jacks used for loading the plate is shown in Fig. 1 (upper). There are 17 jacks; seven of them have single attachment with the plate and the remaining ten are whiffle-tree jacks having two attachments.

The curvature distributions (the $K - S$ plot) of the aerodynamic contour and the plate are shown in Fig. 1 (lower). It may be noted that the curvature of the plate varies linearly between any two-successive jacks. The area shown shaded in this figure represents the slope error between two jacks. The problem of curvature matching consists in selecting the curvatures at the 27 attachments in such a way that the slope-error between any two-successive jacks is zero. This condition gives rise to the following 26 equations connecting $K_1, K_2 \ldots K_{27}$.

$$K_i + K_{i+1} = 2A_{i,i+1}/(S_{i+1} - S_i);\ i = 1,2,\ldots 26 \quad (1)$$

Here $A_{i,i+1}$ is the area under the K-S plot for the aerodynamic contour between ith and $(i + 1)$th jack and is known from the contour design.[1,2,3,4,5]

When the whiffle-tree jacks are used, there are additional constraints on $K_1, K_2 \ldots K_{27}$. These constraints arise as explained below.

Around a typical whiffle-tree jack, we have a curvature distribution as shown in Fig. 2. The following relations hold for the shear force on the plate

$$EIm_j + R_1 = EIm_{(j+1)} \quad (2)$$

$$EIm_{j+1} + R_2 = EIm_{(j+2)} \quad (3)$$

where

$$R_1 + R_2 = R \text{ (Fig. 2)}$$

From these equations we have

$$2EIm_{(j+1)} = EIm_{(j+2)} + EIm_j + (R_1 - R_2) \quad (4)$$

If the linkages for the whiffle-tree jacks are such that $R_1 = R_2 = R/2$, we get a relation connecting the slopes m_j only

$$m_{j+1} = (m_{j+2} + m_j)/2 \quad (5)$$

There are 10 equations of Eq. (5) type.

Equations (1) together with Eq. (5) form a set of simultaneous equations in the unknown K_i. The number of equations is 36.

In a matrix notation these equations can be written as

$$[C] \cdot [K] = [A]$$

A least-square analysis gives

$$[K] = [M]^{-1} \cdot [C]^T \cdot [A]$$

where

$$[M] = [C]^T \cdot [C]$$

Received July 29, 1970. Presented at 22nd Annual Meeting of Aeronautical Society of India, held at Hyderabad on March 20–21, 1970.

* Scientist, Aerodynamics Division.